ARTICLE

OBC
www.rsc.org/obc

Azo dye oxidation with hydrogen peroxide catalysed by manganese 1,4,7-triazacyclononane complexes in aqueous solution

Bruce C. Gilbert,*[a] John R. Lindsay Smith,*[a] Maurice S. Newton,[a] John Oakes[b] and Roger Pons i Prats[a]

[a] *Department of Chemistry, University of York, Heslington, York, UK YO10 5DD*
[b] *Unilever Research, Port Sunlight Laboratories, Bebington, Merseyside, UK L63 3JW*

Received 28th January 2003, Accepted 10th March 2003
First published as an Advance Article on the web 3rd April 2003

A kinetic and mechanistic study is reported of the oxidation of a number of azonaphthol dyes with hydrogen peroxide in aqueous solution, catalysed by some mono and dinuclear manganese(IV) complexes of 1,4,7-trimethyl-1,4,7-triazacyclononane (Me_3TACN). The results of UV-Vis investigations, augmented by EPR and ESI-MS studies, are described for a series of experiments in which concentrations, pH and ionic strength have been varied. The reactions are characterised by an induction period followed by a relatively rapid oxidation. For the dinuclear manganese complex **2**, these are consistent with an initial perhydrolysis of the manganese complex involving both the dye anion and HO_2^-, to give mononuclear manganese species and the operation of a catalytic cycle incorporating $Mn^{III}L(OH)_3$, $O{=}Mn^{V}L(OH)_2$ and $Mn^{IV}L(OH)_3$ (L = Me_3TACN) (*cf*. the reactions of peroxidase enzymes). ESI-MS results provide evidence for the formation and reaction (with the dye) of $Mn^{IV}L(OH)_3$. With the mononuclear manganese complex $Mn^{IV}L(OMe)_3$, there is a short lag-phase attributed to perhydrolysis by HO_2^- followed by the same catalytic cycle.

Introduction

Dinuclear μ-oxo manganese centres appear as subunits in a number of biologically important metalloenzymes, for example in the oxygen evolving centre of photosystem II (OEC)[1] and in catalases.[2] This has stimulated the preparation of a number of dinuclear manganese complexes as models for the enzymes and as potential catalysts.

Some of the dinuclear manganese complexes have been found to exhibit catalase activity with hydrogen peroxide,[3] for example, the first functional and structural model, complex **1**,[4] which contains *N*,*N*,*N*′,*N*′-tetrakis-(2-methylenebenzimidazolyl)-1,3-diaminopropan-2-ol as a bridging heptadentate ligand, a μ-oxo bridge and a μ-carboxylate ligand. This manganese benzimidazolyl complex has a $Mn^{II}Mn^{II}$ oxidation state which is believed to be a model for the resting state of Mn catalase (*L. Plantarum*), although the rate constant for its decomposition of hydrogen peroxide is significantly lower than that of the enzyme. Wieghardt and coworkers[5] have prepared a number of structural models using dinuclear manganese complexes of the ligand 1,4,7-trimethyl-1,4,7-triazacyclononane (Me_3TACN) including the μ-oxo, peroxo and acetate bridged complexes **2**, **3** and **4** respectively. The dinuclear μ-oxo and acetate bridged complexes appear to be good structural models for OEC and catalase and the oxidation level of the manganese centres can be varied from II to IV.[5c]

Enzyme models and other structurally related manganese complexes have received increasing attention in recent years as potential oxidation catalysts. For example, the dinuclear manganese complex **2**, which can typically be used in organic solvents and in aqueous solution at pH <11, catalyses many oxidations with hydrogen peroxide, including stain bleaching,[6] alkene epoxidation[6b,7] and dihydroxylation[8] and the oxidation of alkanes,[9] phenolic substrates,[10] alcohols,[11] sulfides [12] and DNA. [13]

Reactions with manganese complexes **2** and **5** and the related mononuclear complex **6** reported by Hage and coworkers,[6] include the epoxidation of 4-vinylbenzoic acid, (*E*)-4-phenylbut-3-enoic acid and styrene with H_2O_2; the importance of TACN ligands in stabilising reaction intermediates in these oxidations has been stressed.

Other relevant work includes the use of zeolite-based Mn–TACN complexes in the selective epoxidation of alkenes by H_2O_2 (in which Mn^{III}–Mn^{IV} and Mn^{III} complexes have been characterised by EPR spectroscopy)[14] and the use of dinuclear manganese complexes of tris[(pyrid-2-yl)methyl]amine and bis[(6-methylpyrid-2-yl)methyl]ethanediamine in delignification and pulp bleaching catalysis.[15]

Our interest lies in the catalysis mechanisms of **2** and related compounds in oxidation chemistry, and their relationship to those suggested for enzymic systems. We note that high valent oxomanganese species rather than radical-based oxidations have been proposed as the active oxidants in alkene epoxidations carried out with Mn–salen and porphyrin catalysts,[16] and indeed oxomanganese(V) species have been detected in both systems.[17] Further, it has been suggested that oxomanganese intermediates could also be responsible for the epoxidations by Mn complexes with TACN derived ligands.[6a] Barton and coworkers[18] have studied the oxidation of a selection of organic compounds in pyridine–water mixtures, with periodic acid or Oxone, catalysed by **2** and suggest a dinuclear $O{=}Mn^{V}$–Mn^{IV} species as the active oxidant. However, mononuclear high-valent oxo–Mn species could also play an important part in these reactions; indeed we have shown that such an oxomanganese(V) complex is formed in the oxidation of electron-rich phenols catalysed by **2**.[19] Furthermore, the mononuclear Mn complex **6** with a Me_3TACN ligand, exhibits similar catalytic activity to **2** and **5** towards the epoxidation of alkenes.[6a,20] In studies involving the oxidation of phenols catalysed by **2**, we have employed EPR spectroscopy to monitor the formation of phenoxyl radicals (from hindered phenols) as well as the mixed valence $Mn^{III}Mn^{IV}$ complex from the one-electron reduction of **2**[10] (also characterised in the reactions of **2** with catechols[6a]). The importance of 1-electron transfer reactions, as well as the role of H_2O_2 in completing a catalytic cycle, has been stressed.

In the work to be described here, we have investigated the reactions involved in the oxidative bleaching of a series of azo dyes with the dimanganese complex **2** and the mononuclear complex **6** in the presence of H_2O_2 in aqueous solution. Our primary aim was to delineate an overall mechanism, and in particular the factors governing reactivity and catalysis.

DOI: 10.1039/b301026k

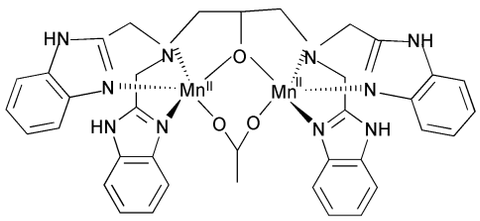

1

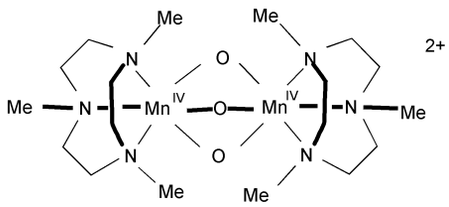

2

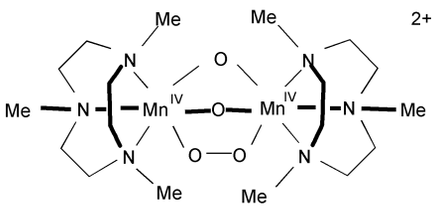

3

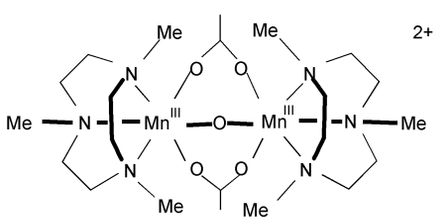

4

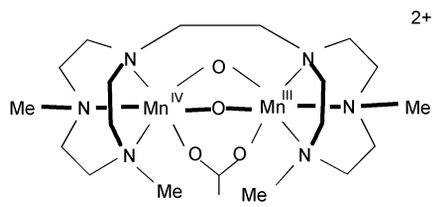

5

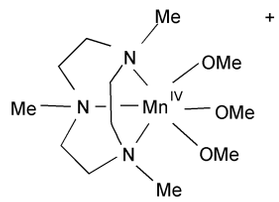

6

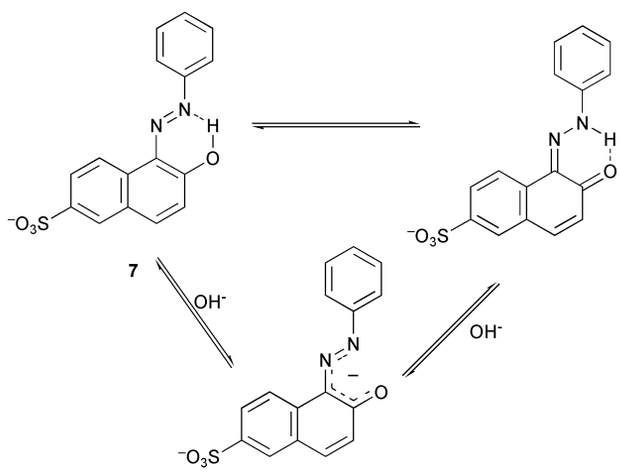

7

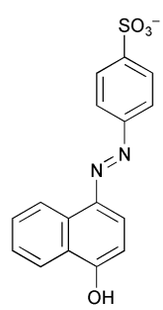

8

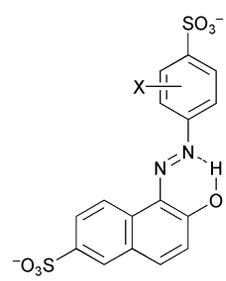

9 **a**, 4-Cl
b, 4-Me
c, 4-$CHMe_2$
d, 2-Me
e, 2-CO_2H
f, 2-SO_3^-
g, 2-OMe

Results and discussion

(1) Oxidation of Acid Orange 12 and related dyes with H_2O_2 catalysed by $[Mn^{IV}(\mu\text{-}O)_3Mn^{IV}(Me_3TACN)_2]^{2+}$ (2)

(a) Kinetic studies of dye bleaching. Our initial approach has been to employ UV–Vis spectroscopy to study the oxidative bleaching of the azo dye Acid Orange 12 (**7**) (λ_{max} 484 nm) with H_2O_2 in the presence of the complex (**2**) in aqueous solution. After initial experiments in which reagent concentrations were varied widely, the following standard conditions were chosen for the majority of our studies: [dye], 2.5×10^{-5}; [**2**], 8×10^{-6}; and $[H_2O_2]$, 9×10^{-3} mol dm^{-3}. We have carried out experiments as a function of pH, typically in the range 2–13, but especially at pH 10–11, with a variety of buffers (borate, carbonate, phosphate and KCl–NaOH) and using a range of ionic strengths.

In most of the experiments the catalysed reactions show three distinct phases, as described in more detail below, namely an initial induction period (lag-phase) followed by a fast phase and finally a slower bleaching (see Fig. 1). In these experiments it was found that pre-mixing any two of the reagents (H_2O_2, **2** or **7**) 20 min before the addition of the third did not decrease the lag phase. From these observations it can be concluded that in the lag-phase the catalyst, dye and H_2O_2 are all involved in the formation of the active species which are responsible for the oxidation of the dye in the fast phase (The identities of these species are discussed in more detail below). Attempts to detect interactions between the dye and $[Mn^{IV}(\mu\text{-}O)_3Mn^{IV}(Me_3TACN)_2]^{2+}$ or hydrogen peroxide by UV–Vis spectroscopy were unsuccessful, although the latter combination led to a very slow uncatalysed bleaching of the dye by hydrogen peroxide.[21]

(b) Effect of buffer, buffer concentration, ionic strength and pH. With carbonate buffer (pH 10.1) and constant ionic strength (0.035, adjusted with NaCl), the effect of variation in the buffer concentration is negligible. Interestingly, under the same conditions with borate buffer, the reaction is sensitive to the buffer concentration; the lag-phase increases and the fast

phase slows down as the concentration is increased. The origin of this difference in buffer behaviour is unclear. Experiments with either buffer system in which the ionic strength was increased (with NaCl) from 0.015 to 0.15 also led to an increase in the lag-phase and a retardation of the fast phase of the reaction (Fig. 1). Comparable results were obtained when the ionic strength was adjusted with $NaNO_3$. These results suggest that both the lag-phase and the fast phase involve the reaction of species of opposite charge, for example the dye anion or HO_2^- and a positively charged manganese complex.

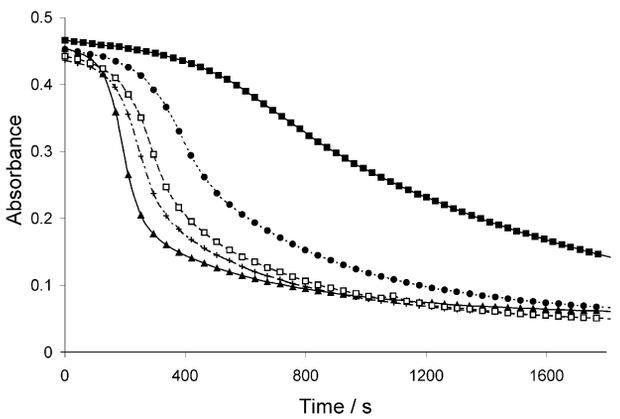

Fig. 1 Dependence of absorbance time plots on ionic strength (NaCl) in the oxidation of dye **7**, in aqueous carbonate buffer (pH 10.0), with hydrogen peroxide catalysed by **2**. Ionic strength, ■ 0.15; ● 0.06; □ 0.04; + 0.03; ▲ 0.015. ([dye], 2.5×10^{-5}; $[H_2O_2]$, 9×10^{-3}; [**2**] 8×10^{-6} mol dm^{-3}).

The next set of experiments involved variations of pH. Figs. 2 and 3 illustrate the typical findings. From the former it can be seen that the lag phase becomes significantly reduced at pH > *ca.* 10 and appears to mirror the ionisation of the dye to its anion. Thus, at low pH only a small % of dye is ionised which in turn results in a long lag-phase, whereas at pH values above the dye's pK_a (10.8 [22]) the lag-phase almost disappears as the majority of the dye is ionised.

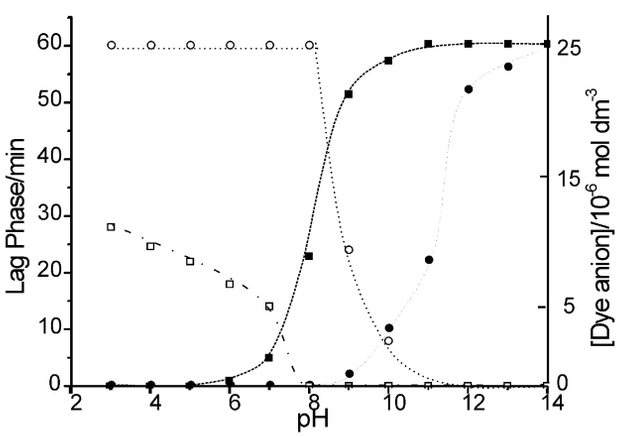

Fig. 2 Dependence of the length of the lag-phase and dye anion concentration on pH. For dye **7**, ○ lag-phase and ● anion concentration; for dye **8**, □ lag-phase and ■ anion concentration. ([Dye], 2.5×10^{-5}; $[H_2O_2]$, 9×10^{-3}; [**2**] 8×10^{-6} mol dm^{-3}).

Fig. 3 shows a plot of the maximum rate of the rapid reaction phase *versus* pH from experiments in which both the pH and the buffer were varied. The maximum reaction rate reaches a peak at pH *ca.* 10.5. This might again reflect in part the more rapid oxidation of the anion of **7** or alternatively the ionisation of H_2O_2 (pK_a 11.6). The decrease in the maximum rate at high pHs can be attributed to catalyst decomposition.

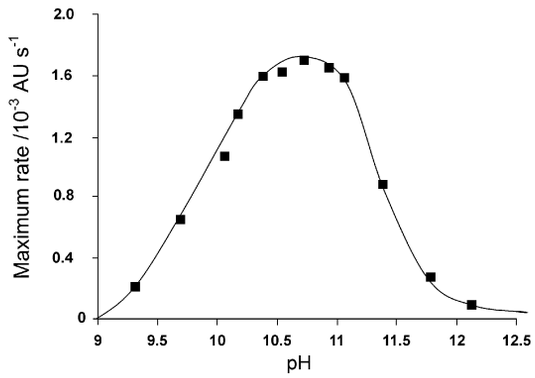

Fig. 3 Dependence of the maximum rate of bleaching of dye **7** (λ 484 nm) on pH, in aqueous carbonate buffer (pH 10.0), with hydrogen peroxide catalysed by **2**. ([Dye], 2.5×10^{-5}; $[H_2O_2]$, 9×10^{-3}; [**2**] 8×10^{-6} mol dm^{-3}).

The pH dependence of the lag phase and the maximum rate of reaction were investigated further in parallel experiments with the related azo dye Orange I (**8**). Since the hydroxyl group in (**8**) is not adjacent to the azo linkage, there is no intramolecular hydrogen-bond between these groups and the pK_a of this dye (pK_a 8.11) [22] is much lower than that of **7**. In agreement with the conclusions above, the lag-phase disappears once most of the dye is ionised (pH > 9.0, Fig. 2). On the other hand, the maximum rate of the rapid phase of the reaction shows an almost identical pH profile to **7** suggesting that, although the dye anion is likely to be the substrate, the increase in rate observed between pH 8 and 11 arises from the ionisation of H_2O_2 rather than that of the dye.

(c) Variation in the concentration of H_2O_2, dye and catalyst: effects on the lag-phase and the rate of dye bleaching. These experiments were largely conducted using the standard conditions (see above) with carbonate buffer at pH 10.1. Some experiments were also carried out with borate buffer under comparable conditions.

(i) Variation in [H_2O_2]. At H_2O_2 concentrations < 3×10^{-3} mol dm^{-3} ($[H_2O_2]$: [cat] < 400), the maximum rate of bleaching of **7** appears to be directly proportional to $[H_2O_2]$ (Fig. 4a). However, at higher concentrations (3×10^{-3} to 2.8×10^{-2} mol dm^{-3}) the effect is dramatically attenuated suggesting that a very large excess of hydrogen peroxide over catalyst leads to saturation kinetics or catalyst destruction.

(ii) Variation in [dye]. With other concentrations held constant, increasing that of the dye shortens the lag-phase and increases the rate of oxidation (as judged by the maximum slope of the absorbance time plots). Fig. 4b shows that the maximum slope is linearly dependent on [dye]. We conclude that the dye is involved in the build-up of an active species in the lag-phase (discussed further below) and also, as would be expected in the bleaching–oxidation process itself.

(iii) Variation in [catalyst]. Increasing the catalyst concentration leads to both a marked decrease in the lag-phase and an increase in the maximum rate of reaction. As described above for the rate variation with [dye], the maximum rate is linearly dependent on [catalyst] (Fig. 4c). These results show that, as expected, the catalyst is involved in the reactions occurring during the lag-phase and in the rapid oxidation process itself.

(d) The influence of EDTA and Me_3TACN. The oxidation of Acid Orange 12 (**7**), under the standard conditions in carbonate buffer at pH 10.1, was investigated in the presence of the two ligands, EDTA and Me_3TACN. The inclusion of one equivalent of EDTA in the reaction mixture has a dramatic inhibitory effect on the dye bleaching. We conclude that EDTA complexes the manganese and effectively removes it from the catalytic cycle.

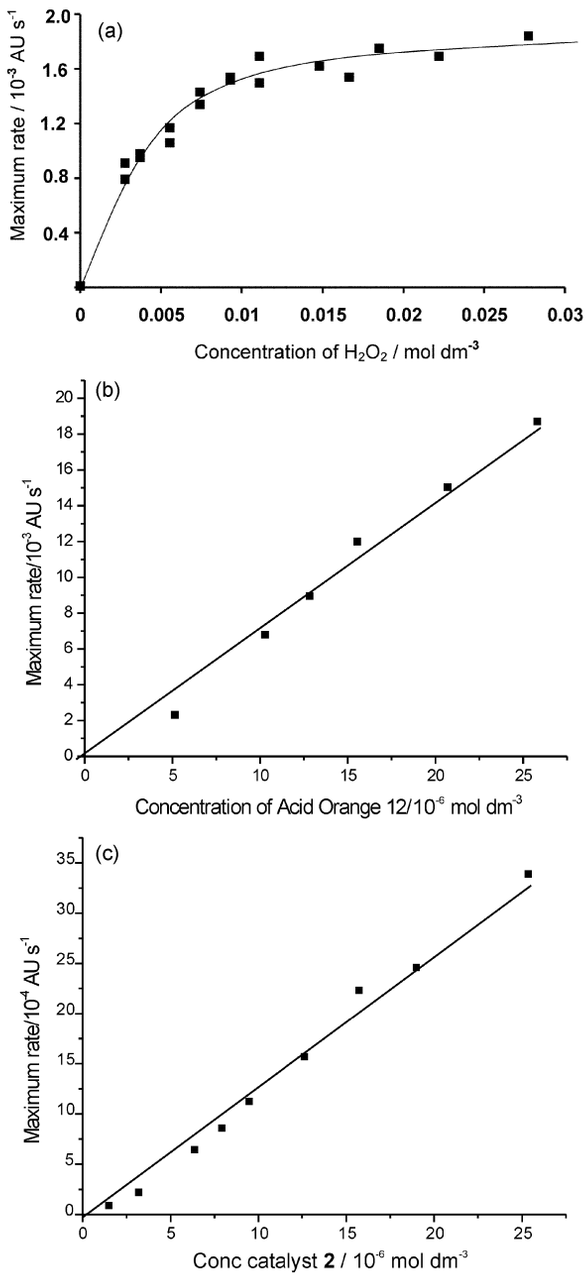

Fig. 4 Dependence of the maximum rate of bleaching of dye **7** (λ 484 nm), in aqueous carbonate buffer (pH 10.0) with hydrogen peroxide catalysed by **2**, on the concentration of (a) hydrogen peroxide; [dye], 2.5×10^{-5}; [**2**] 8×10^{-6} mol dm^{-3}; (b) dye; [H_2O_2], 9×10^{-3}; [**2**] 8×10^{-6} mol dm^{-3}; (c) catalyst; [dye], 2.5×10^{-5}; [H_2O_2], 9×10^{-3} mol dm^{-3}.

In contrast, the presence of 1–7 equivalents of the Me_3TACN ligand has little effect on the maximum rate of bleaching although interestingly there is a very marked lengthening of the lag phase with increasing [Me_3MTACN]. The possibility that Me_3TACN complexes the manganese as an inactive Mn(Me_3-MTACN)$_2$ species was rejected. Such a complex might account for an increased lag-phase but it would also retard the fast phase of the reaction. ESI-MS studies of reactions using a high ratio of Me_3TACN to **2** provided no evidence to support the formation of such a species. An alternative explanation is that the excess ligand acts as a competitive substrate diverting the active oxidant from dye bleaching. Once its concentration has been reduced by oxidation, dye bleaching can proceed as normal. (ESI-MS studies which provide clear evidence for ligand oxidation are discussed below). The precise cause of the inhibitory effect of added Me_3TACN in these oxidations is currently under investigation.

(e) The oxidation of azo dyes structurally related to Acid Orange 12. To explore the effect of the structure of the dye on the lag-phase and the maximum rate of reaction, we investigated the nine 1-arylazo-2-naphthol-6-sulfonates (**7**), (**9a**–**g**) and Calmagite [1-(2-hydroxy-5-methylphenylazo)-2-naphthol-6-sulfonate] (**10**) as well as Orange I (**8**) [1-(4-sulfonatophenylazo)-4-naphthol] (described above), Orange II [1-(4-sulfonatophenylazo)-2-naphthol] (**11**) and the *O*- and *N*-methylated compounds **12** and **13**. The 1-arylazo-2-naphthol azo dyes (**9**) were, in particular, selected to carry out a systematic investigation of substituent electronic and steric effects on the lag-phase.

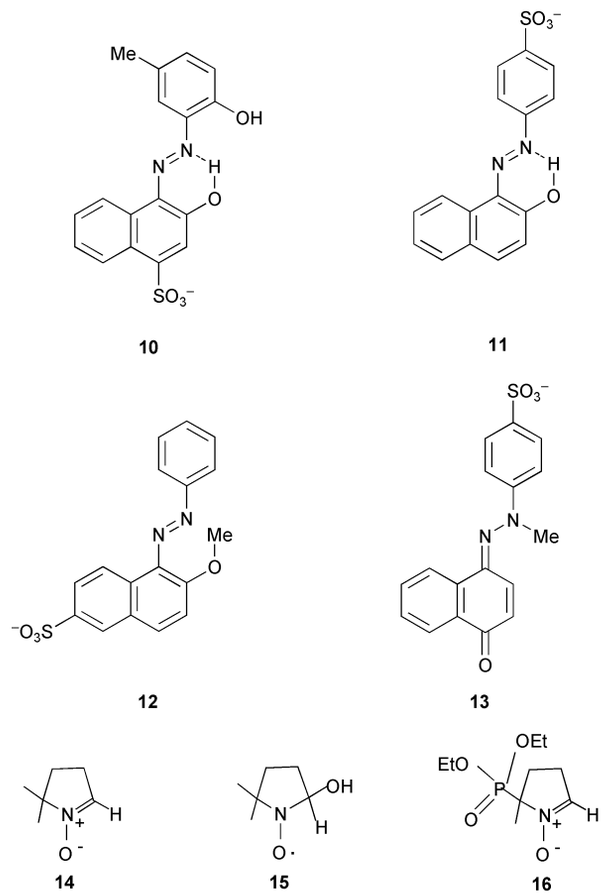

With the exception of Calmagite, all the 2-naphthol dyes, (**7**,**9a**–**g and 11**, pK_a values in the range 10.5–12),[22] where the hydroxyl group is positioned adjacent to the azo linkage, show a lag-phase at pH 10. However, as noted above, at this pH Orange I (**8**) (pK_a 8.11) shows essentially no lag-phase, supporting the conclusion that the dyes need to be ionised prior to reaction with **2**. Calmagite which is a relatively easily oxidised diphenol (pK_a 8.4 and 12.7)[23] and a strong ligand for manganese(II)[24] reacts directly with **2** in the absence of H_2O_2, presumably by the electron-transfer mechanism we reported previously.[10] A study of the reaction profiles for the five 1-(2-substituted phenylazo)-2-naphthol dyes (**7**,**9a**–**g**) in their oxidations with H_2O_2 and **2** (Fig. 5) reveals no apparent correlation of the lag-phase or the maximum rate with dye pK_a: for example the 2-CO_2H and 2-SO_3H substituted dyes have very similar pK_a values[22] but very different reaction profiles; the former has a significantly shorter lag-phase and faster maximum rate of bleaching. These results suggest that substituent steric effects and metal-binding properties may be important. The catalyst, by ligating to the carboxylate group, may reduce the lag-phase by aiding the breakdown of **2** to give the active oxidant.

The lag-phases in the oxidations of the 1-(4-substituted arylazo)-2-naphthol-6-sulfonate dyes (**7**,**9a**–**c**) are all very similar, leading to the conclusion that the influence of the electronic

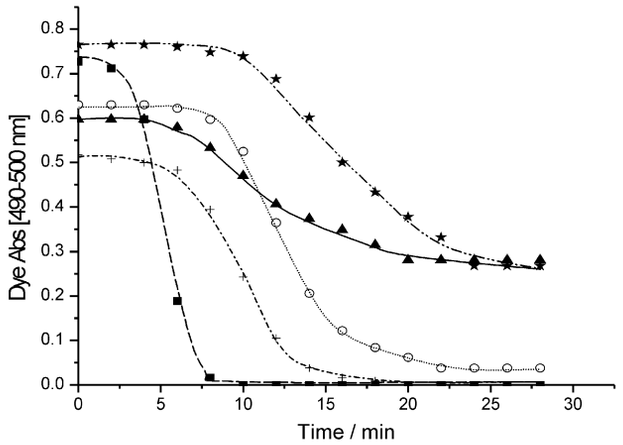

Fig. 5 Absorption *versus* time plots for the oxidation of dyes **7** and **9d**–**g** by hydrogen peroxide catalysed by **2** in aqueous solution, pH 10.0. + dye **7**; ○ dye **9d**; ■ dye **9e**; ▲ dye **9f**; ★ dye **9g**. ([Dye], 2.5×10^{-5}; [H_2O_2], 9×10^{-3}; [**2**] 8×10^{-6} mol dm^{-3}).

effects, of substituents on the aryl group on the length of the lag-phase is insignificant.

In the final experiments in this category, we investigated the oxidation of *O*- and *N*-methylated dyes (**12** and **13**) in which ionisation, as well as the azo-dye's tautomeric equilibrium (hydrazone *vs* azo structure) is prevented. For the former, no reaction with **2** and/or H_2O_2 was seen. Whereas with the latter, reaction with **2** and H_2O_2 was only observed at pH > *ca* 12. The latter reaction is attributable to the uncatalysed oxidation of **13** by HO_2^-.[22] These results support the conclusion that the dye anions are the substrates in these catalysed oxidations and that the active oxidant is electrophilic rather than nucleophilic.

(f) Measurement of H_2O_2 decomposition in the oxidation of Acid Orange 12 catalysed by $[Mn^{IV}(\mu\text{-}O)_3Mn^{IV}(Me_3TACN)_2]^{2+}$. The reaction between the Acid Orange 12, **2** and H_2O_2 leads to dioxygen evolution as well as dye bleaching. A method was developed in this study to monitor the H_2O_2 concentration, by removing aliquots from the reaction under study in the UV–Vis spectrometer. This enabled both the dye bleaching and H_2O_2 consumption to be followed for a given oxidation and showed that both have very similar reaction profiles (see Fig. 6). No significant decomposition was noted in the absence of the dye over *ca* 60 min suggesting that the active species formed during the lag-phase catalyses the oxidation of both the AO12 dye and hydrogen peroxide. Furthermore, there is a linear relationship between H_2O_2 consumption and the extent of dye bleaching which reveals that ~115 equivalents of H_2O_2 are destroyed during the oxidation of one equivalent of AO12, showing that

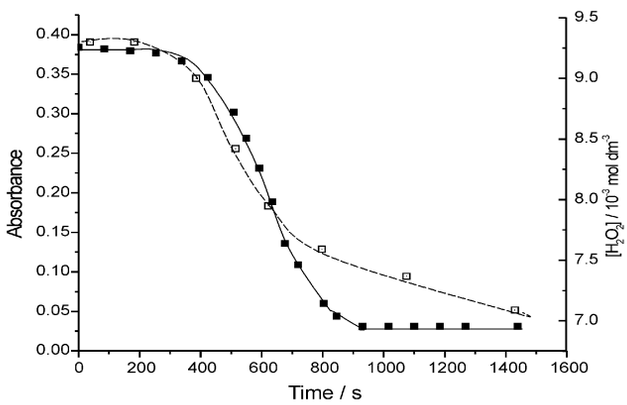

Fig. 6 Decrease in the absorbance of dye **7** (■) (λ 484 nm, right axis) and concentration of hydrogen peroxide (□) (left axis) with time in the oxidation of **7** with H_2O_2 catalysed by **2** in aqueous borate buffer, pH 10.0. ([Dye], 2.5×10^{-5}; [H_2O_2], 9×10^{-3}; [**2**] 8×10^{-6} mol dm^{-3}).

the catalysed decomposition of H_2O_2 to H_2O and O_2 (catalase reaction) and not dye bleaching is the major pathway in these systems.

(g) Stability of the catalyst 2 under the reaction conditions employed. The stability of **2** under the reaction conditions was examined by repeated additions of dye and H_2O_2 to a solution of **2** at pH 10. As a control experiment, the catalytic activity of Mn^{2+} ion, from aqueous $MnSO_4$, was also investigated under the same conditions. These experiments reveal that no lag-phase is observed for the second and subsequent additions of dye–H_2O_2 to the reaction mixtures involving **2**; furthermore the profiles of the repeat oxidations become very similar to those of aqueous Mn^{2+} suggesting that the manganese complexes are effectively destroyed after the second addition of dye and H_2O_2.

(h) EPR spectroscopy and ESI-MS studies. To explore the possibility that free radicals (*e.g.* $^{\bullet}OH$) are produced in the reactions described above and to provide information about potential electron-transfer steps (NB dinuclear Mn^{III}–Mn^{IV} complexes have very characteristic EPR spectra when immobilised in solid matrices),[14] we next employed EPR spectroscopic studies using both spin-trapping and mix-freeze techniques (*cf*. ref 10).

In the spin-trapping experiments we mixed the dye, the spin trap DMPO (**14**), H_2O_2 and the catalyst **2** typically in concentrations ranges $2.5–10 \times 10^{-5}$, $5–10 \times 10^{-2}$, 10^{-2} and $1–10 \times 10^{-5}$ mol dm^{-3}, respectively. Only an extremely weak signal from the corresponding hydroxyl radical–adduct (**15**) was obtained; an observation which most likely reflects either the occurrence of nucleophilic attack of water–hydroxide on the trap, followed by oxidation of the appropriate hydroxylamine (the so-called Forrester–Hepburn mechanism)[25] or metal-mediated oxidation of the trap followed by attack of the nucleophile rather than the trapping of $^{\bullet}OH$.[26] Similar weak signals were also obtained in the absence of dye and/or peroxide. With the trap DEPMPO (**16**), a good trap for $^{\bullet}OH$ or $^{\bullet}O_2H$,[27] only very weak signals characteristic of metal-ion oxidation of the trap itself were obtained.[28] We conclude that neither $^{\bullet}OH$ nor $^{\bullet}O_2H$ is formed in significant quantities during the reaction of dye, H_2O_2 and catalyst **2**.

In mix and freeze experiments, aliquots were removed at regular time intervals from reactions, of the dye **7** or **8**, H_2O_2 and catalyst **2** (with concentrations 0.68×10^{-3}, 0.4 and 0.7×10^{-3} mol dm^{-3}, respectively) at pH 10 or 11.5 in borate buffer (0.01 mol dm^{-3}); these were mixed with MeOH and frozen at 77 K. No significant signals attributable to the species $[Mn^{III}(\mu\text{-}O)_3Mn^{IV}(Me_3TACN)_2]^{+}$, which shows a characteristic 16-line spectrum,[6,10] were detected in these experiments or in the mixing of **2** with either of the dyes or H_2O_2. We conclude that the reaction does not involve the one-electron reduction of **2**.

Electrospray ionisation-mass spectrometry (ESI-MS) experiments were carried out on aqueous solutions of **2** as well as mixtures of **2** with H_2O_2 and/or dye **7** using conditions similar to those of the UV–Vis experiments described above (typically pH 10, 30 °C with [dye], **2**, and H_2O_2, 2.5×10^{-5}, 8×10^{-6} and 9×10^{-3} mol dm^{-3}). The dominant peak in the spectrum from **2** is at *m*/*z* 645 with a minor peak at *m*/*z* 250, consistent with monocationic $[Mn^{IV}(\mu\text{-}O)_3Mn^{IV}(Me_3TACN)_2]^{2+}(PF_6)^{1-}$ and the dicationic species $[Mn^{IV}(\mu\text{-}O)_3Mn^{IV}(Me_3TACN)_2]^{2+}$ respectively. A similar spectrum was obtained from a mixture of **2** and H_2O_2 indicating that under these conditions the dinuclear structure of **2** remains intact. Addition of the azo dye **7** to this mixture led to the detection, after one minute (a time period within the lag-phase), of many new signals (*e.g. m*/*z* 277, 259, 243, 229). These new species are characterised as the following mononuclear Mn complexes by assigning their overall charge and on the basis of applying tandem mass spectrometry (MS–MS): *m*/*z* 277, $[(Me_3TACN)Mn^{IV}(OH)_3]^{+}$; *m*/*z* 259,

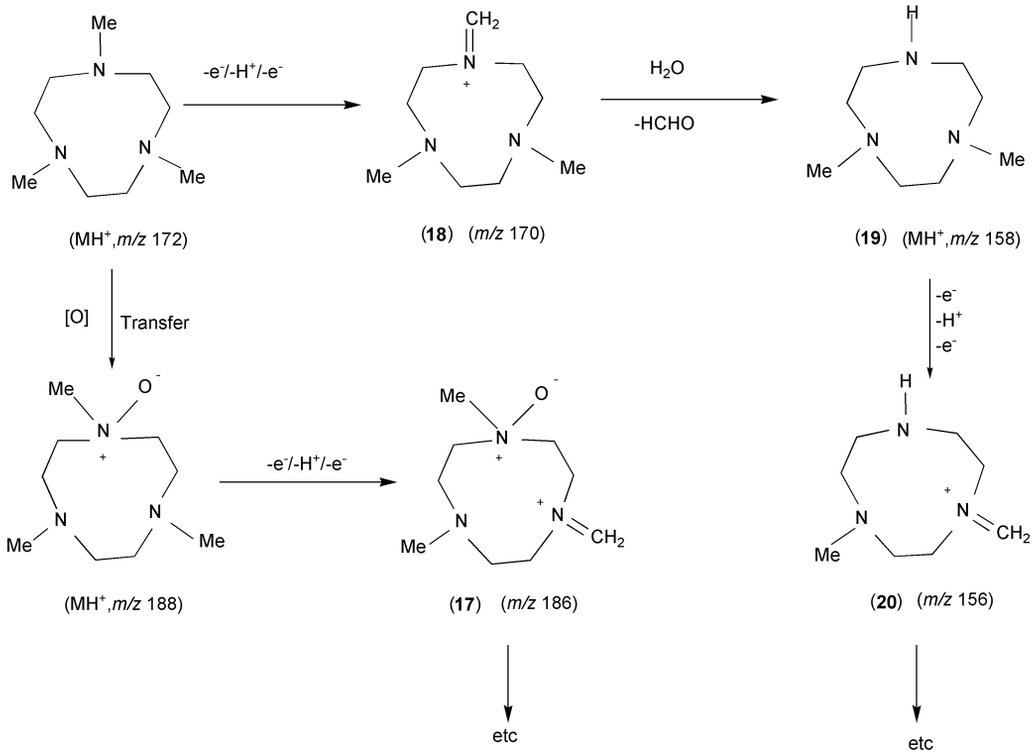

Scheme 1 Oxidative degradation of the Me_3MTACN ligand.

$[(Me_3TACN)O{=}Mn^{IV}(OH)]^+$; *m/z* 243, $[(Me_3TACN)Mn^{II}(OH)]^+$ and *m/z* 229, $[(Me_2TACN)Mn^{II}(OH)]^+$. In the last species the Me_3TACN ligand has been oxidatively demethylated at one position (see below). It is likely that this occurs by oxidation of free ligand, formed in catalyst degradation, followed by Me_2TACN–Me_3TACN ligand exchange. Ligand exchange rates in manganese complexes are dependent on the ligand type and the oxidation state of the manganese; they are dramatically faster in Mn(II) and Mn(III) than Mn(IV) complexes.[1b]

The ESI-MS results reveal that during the lag-phase of the reaction there is little change in the relative intensities of the ESI-MS signals assigned to the dinuclear manganese complex **2** (*m/z* 645) and mononuclear $[(Me_3TACN)Mn^{IV}(OH)_3]^+$ (*m/z* 277). Following the lag-phase, the peak characteristic of the mononuclear species increases to a maximum at the expense of the dinuclear species. This corresponds to the fast phase of the reaction. In the final phase, the intensities of all the ions from the mono- and di-nuclear manganese intermediates decrease and breakdown products of these complexes, with *m/z* 186, 172, 170, 158 and 156, are detected. The ion with *m/z* 172 is assigned to the protonated free ligand, Me_3TACNH^+ and *m/z* 186, 170, 158 and 156 are attributable to products (**17**–**20**) from ligand degradation. These results show that reaction of **2** with H_2O_2 is capable of bringing about both one-electron oxidative demethylation (*m/z* 170, 158 and 156)[28] and oxygen-transfer (*m/z* 186) (Scheme 1). Both types of reaction have been noted previously with **2**, the former in the oxidation of phenols[10] and the latter in the epoxidation of alkenes[6b,7] and the formation of sulfoxides from sulfides.[12] The relative importance of these two pathways in oxidations will depend on the nature of the substrate, and in particular on its oxidation potential.

The results from the ESI-MS experiments suggest that mononuclear manganese species play an important role in the dye oxidation; for example, the catalytic activity (**7** decolorisation) increases only after the concentration of the mononuclear $[(Me_3TACN)Mn^{IV}(OH)_3]^+$ species also increases. Thus we can conclude that, in the presence of Acid Orange 12 and H_2O_2, (**2**) breaks down into mononuclear Mn species including $[(Me_3TACN)Mn^{IV}(OH)_3]^+$ (*m/z* = 277). The correlation between the concentration of $[(Me_3TACN)Mn^{IV}(OH)_3]^+$ and dye decolorisation suggests that this Mn-intermediate plays a key role in the dye oxidation (see below).

(2) Oxidation of Acid Orange 12 with H_2O_2 catalysed by $[(Me_3TACN)Mn^{IV}(OMe)_3]^+$ (6)

In order to explore the behaviour of an analogous mononuclear manganese Me_3TACN complex with H_2O_2 and the dye (**7**), we carried out a related set of investigations catalysed by **6**, a catalyst previously studied by Hage and coworkers.[6,20] The kinetics of the oxidative bleaching were followed under the standard conditions by UV-Vis spectroscopy, as described above.

Fig. 7 compares the reaction profiles of the **6**- and the **2**-catalysed decolorisation of **7** by H_2O_2 at pH 10 in borate buffer. Both show a lag-phase followed by an increased oxidation rate; however, the inflection point in the curve for the reaction of **6** is less sharp, and its lag-phase is shorter than that

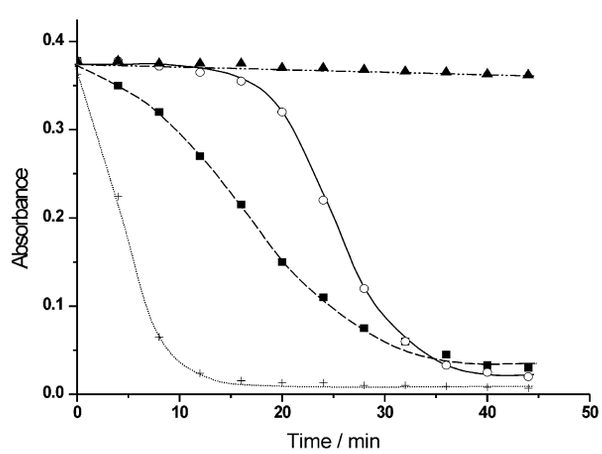

Fig. 7 Comparison of absorption (λ 484 nm) *versus* time plots for the oxidation of dye **7** with hydrogen peroxide in aqueous borate buffer, pH 10.0, ▲ uncatalysed; ○ catalysed by **2**; ■ catalysed by **6**; + catalysed by $MnSO_4$ and Me_3TACN. ([Dye], 2.5×10^{-5}; $[H_2O_2]$, 9×10^{-3}; [**2**] and [**6**] 8×10^{-6} and $[MnSO_4]$–Me_3TACN 16×10^{-6} mol dm^{-3}).

for **2**. The lag-phase was unchanged when **6** was pre-incubated with **7**, but preincubation of **6** with H_2O_2 resulted in a shorter lag-phase, suggesting that reaction between H_2O_2 and **6** may also be generating a key active species.

The pH dependence of the maximum rate of the **6**-catalysed oxidation of **7** (Fig. 8) parallels that of the dinuclear analogue **2**: the increase in rate over the pH range 9–11 is attributed to the importance of HO_2^- as a reactant and the decrease in rate at higher pHs is attributed to catalyst decomposition at high pH. The oxidative stability of **6** was also investigated, at pH 10, by repeated additions of H_2O_2 and **7**. As noted above for reactions catalysed by **2**, no lag-phase is observed following the second addition of **7** and H_2O_2 and the catalyst is effectively converted to manganese oxides or hydroxides in the third and subsequent oxidations.

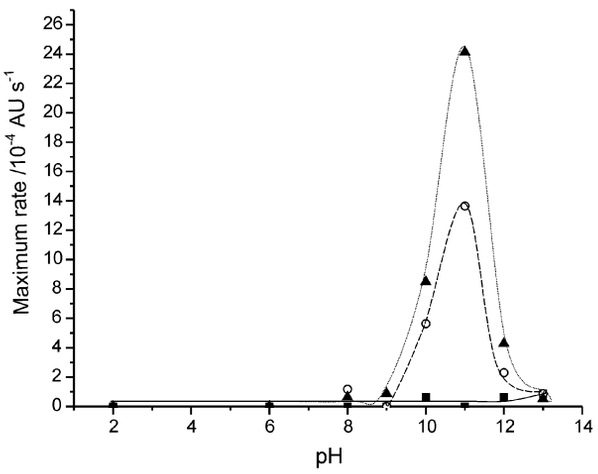

Fig. 8 Dependence of the maximum rate of bleaching of dye **7** (λ 484 nm) on pH, in aqueous borate buffer (pH 10.0), with hydrogen peroxide, ■ uncatalysed; ▲ catalysed by **2**; ○ catalysed by **6**. ([Dye], 2.5×10^{-5}; [H_2O_2], 9×10^{-3}; [**2**] 8×10^{-6} mol dm^{-3}).

The consumption of H_2O_2 at pH 10, by the mononuclear complex **6** in the presence and absence of **7** shows that the dye increases the rate of hydrogen peroxide decomposition, presumably because it is involved in the catalytic cycle, with H_2O_2–HO_2^- and **6**, which promotes the turnover of the active Mn species. Decomposition of H_2O_2, during the **6**-catalysed oxidation of **7**, was also followed at pH 7 and 10 and the reaction profiles for H_2O_2 consumption are very similar to the corresponding profiles for dye bleaching. The highest oxidation rates for H_2O_2 and dye decomposition are found at pH *ca*. 11 (see above), suggesting that the same mononuclear manganese species is responsible for the decomposition of both **7** and H_2O_2 in related experiments with both **2** and **6**. This species is most active in the pH range 9.5–11.5. Mn oxides, formed from the decomposition of manganese complexes above pH 11, do not appear to contribute significantly to the decomposition of either **7** or H_2O_2.

Using EPR spectroscopy we were unable to detect $Mn^{III}Mn^{IV}$ species in reaction solutions, of **6** with either or both **7** and H_2O_2, frozen shortly after mixing. ESI-MS analysis of solutions of **6** at pH 10 gave two dominant peaks with *m/z* 319 and 243 which are assigned to **6** and $[(TMTACN)Mn^{II}(OH)]^+$ respectively. The addition of H_2O_2 led to the rapid formation of a new peak at *m/z* 277, assigned the structure $[(Me_3TACN)Mn^{IV}(OH)_3]^+$, evidently formed in the perhydrolysis of **6**. A similar result was observed when this reaction was repeated in the presence of **7**. The kinetic profile for these peaks (Fig. 9, recorded for the oxidation of **7** under standard conditions) reveals a timescale for 'perhydrolysis' (and subsequent decomposition of $[(Me_3TACN)Mn^{IV}(OH)_3]^+$) which relates closely to the dye oxidation behaviour (Fig. 7).

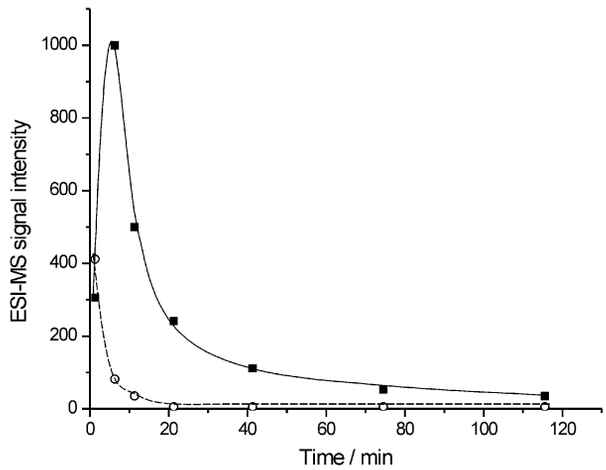

Fig. 9 Intensities of the ESI-MS peaks with *m/z* 319 (○) and 277 (■) as a function of time in the oxidation of **7** with hydrogen peroxide catalysed by **6** in aqueous borate buffer, pH 10.0. ([Dye], 2.5×10^{-5}; [H_2O_2], 9×10^{-3}; [**2**] 2.7×10^{-5} mol dm^{-3}).

(3) Oxidation of Acid Orange 12 with H_2O_2 in the presence of manganese(II) ions and Me_3TACN

A series of experiments was undertaken to test whether or not the active mononuclear manganese Me_3TACN complexes, found in reactions of **2** and **6** could also be generated *in situ* in reaction mixtures from Mn^{II}, Me_3TACN and H_2O_2. Kinetic studies on the reaction of **7** with the *in situ* system, under the standard conditions, showed that oxidative bleaching occurs without a lag-phase with a maximum rate very comparable to that with the dinuclear catalyst (**2**) (Fig. 7). ESI-MS analysis also showed that the addition of H_2O_2 to a mixture of Me_3TACN and $MnCl_2$, in aqueous carbonate buffer at pH 10.0, gave the species with *m/z* 277, $[(Me_3TACN)Mn^{IV}(OH)_3]^+$ observed in the reactions of **2** and **6**.

(4) Mechanistic conclusions

The results described above establish that the anion of the dye, HO_2^- and the catalyst **2** all play an important role in the overall oxidation reaction and that their presence and concentrations affect the length of the lag-phase and the rate of the rapid phase of the reactions. No evidence for $[Mn^{III}(\mu\text{-}O)_3Mn^{IV}(Me_3TACN)_2]^+$ which would be formed by one-electron reduction of **2** has been obtained; it is noteworthy that this species is a key intermediate in the reactions of electron-rich phenols with **2**, both in the presence and absence of H_2O_2.[10] The redox potentials Acid Orange 12 and its anion have recently been measured by pulse radiolysis techniques and reported to be 0.70 and 0.46 V (*vs*. SCE),[29] the appropriate value of the dinuclear manganese complex **2** has been found to be 0.18 V (*vs*. SCE) at pH 9.5.[30] Given these results, the lack of direct electron-transfer between dye–dye$^-$ and $[Mn^{IV}(\mu\text{-}O)_3Mn^{IV}(Me_3TACN)_2]^{2+}$ is not surprising.

One-electron transfer mechanisms between hydrogen peroxide and manganese complexes are believed to occur mainly through an inner-sphere complex formation because of thermodynamic barriers,[31] for example, in oxidation reactions of H_2O_2 with manganese compounds such as $[Mn^{III}(CDTA)(H_2O)]^-$ (H_4CDTA, cyclohexane-1,2-diyldinitrilotetraacetic acid),[32] $[Mn^{III}(bipy)_2(H_2O)(OH)]^{2+}$ [33] and $Mn^{3+}(aq)$.[34] In addition, manganese triazacyclononane complexes, in which the manganese ions are chelated in a hexadentate fashion, are reported to catalyse H_2O_2 decomposition only if at least one of the ligand arms in the complex becomes detached from the manganese ion to open up a free coordination site for an incoming peroxide or substrate molecule.[7] The importance of a free manganese coordination site may account for why a lag-phase is observed for H_2O_2 decomposition in the presence of **2** and

dye. No reaction takes place between **2** and H_2O_2 at the beginning of the reaction because no free coordination sites are available on the manganese complex. During the lag-phase, a reaction between the dye anion and **2** generates a species (identified as **X** in Scheme 2) which is capable of reacting with hydrogen peroxide. Since **X** cannot be detected by UV-Vis spectroscopy, it is envisaged as being in low concentration, probably in an unfavourable equilibrium with **2** and dye^-.

ESI-MS analyses of the oxidation mixtures identifies $[(Me_3TACN)Mn^{IV}(OH)_3]^+$ as a key intermediate which builds up in the lag-phase and reaches a maximum concentration in the fast phase. This suggests that the reaction of the dye anion, **2** and HO_2^- leads to the breakdown of the dinuclear manganese complex **2** to give reactive mononuclear manganese species. Whether these are manganese(III) or manganese(IV) species remains unclear, however, they are subsequently involved in the oxidation of both the dye and hydrogen peroxide (Scheme 2). A catalytic oxidation cycle that includes a two-electron oxidation of a mononuclear Mn(III) to O=Mn(V) by H_2O_2 followed by two one-electron reductions by the dye anion to regenerate Mn(III), *via* the Mn(IV) species above, is consistent with the data. The same catalytic cycle, after a much reduced or non-existent lag-phase, is also involved in the reactions using the mononuclear catalyst, (**6**), and the *in situ* system respectively.

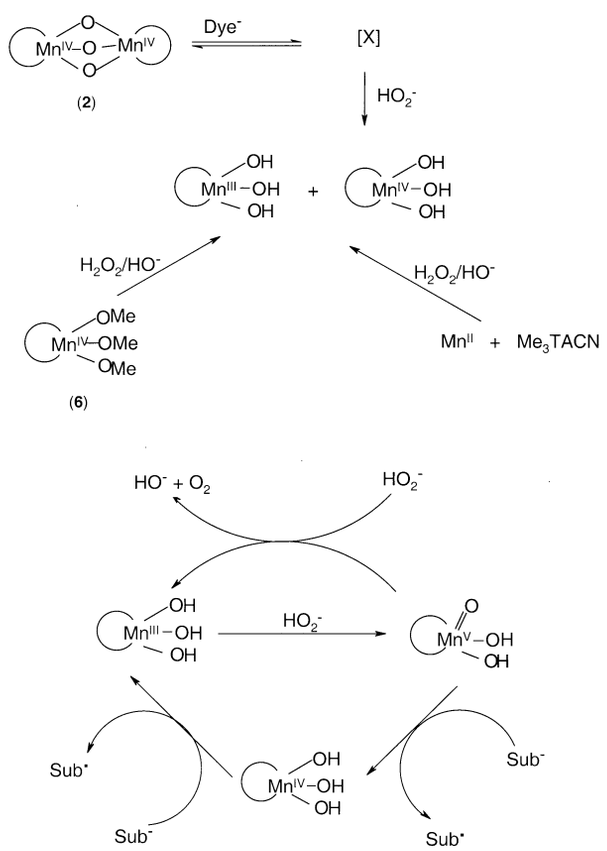

Scheme 2 Oxidation cycles for dye bleaching by H_2O_2 and complexes **2** and **6**

Since EDTA does not react with complex **2** in the aqueous basic solution, we attribute the strong inhibitory effect of this ligand on the oxidations to its ability to remove manganese from one or more of the mononuclear manganese intermediates to give inactive Mn–EDTA chelate complexes.

The use of the catalyst in repeat oxidations shows, as expected, that once the dinuclear complex **2** has been converted into mononuclear manganese species repeat reactions no longer show a lag-phase. However, it also reveals that the catalyst in this system completes relatively few turnovers, based on dye bleaching, before it self-destructs to give metal-free ligand and oxidised ligand.

Scheme 2 closely parallels the general mechanism for oxidations with H_2O_2 catalysed by a peroxidase enzyme: the O=Mn(V) and O=Mn(IV) species correspond to the oxo–iron active oxidants, Compounds I and II, respectively and, as is observed with these species, the O=Mn(V) complex is expected to be a more powerful oxidant than O=Mn(IV).[35] Unfortunately the ESI-MS experiments provided no evidence for the presence of the Mn(III) or O=Mn(V) species in these dye oxidations. The former, which equates to the resting state of the enzyme, being uncharged is ESI-MS silent whereas the latter is too short-lived to be detected. It is noteworthy, however, that in the oxidation of electron-rich phenols with H_2O_2 catalysed by **2** the equivalent mononuclear O=Mn(V) species is sufficiently stabilised in a Me_3TACN–biphenol mixed ligand complex for it to be detected by ESI-MS.[19]

The strong similarity of the reaction profiles of dye bleaching and H_2O_2 depletion is consistent with both H_2O_2 and dye competing for the active oxidant. Interestingly, however, when the large excess of H_2O_2 over dye (360 : 1) is taken into account, the high consumption of H_2O_2 relative to dye oxidation equates to a relatively small selectivity (~3 : 1) by the active oxidant for H_2O_2 over dye. Since we found no evidence for oxy-radicals in these systems, it is likely that a catalase mechanism is operative for the catalysed self-degradation of H_2O_2[36] with the Compound I analogue reacting with HO_2^- to give dioxygen and OH^- (Scheme 2).

To account for the detection of mononuclear manganese(IV) species from the reaction of complex **2** in the present study, the oxidation of the azo dye anion is shown in Scheme 2 as occurring by a single electron-transfer (SET) process rather than oxygen-transfer. Azo dyes are known to be oxidised by both electron- and oxygen-transfer mechanisms; peroxyacids give azoxy derivatives by oxygen-transfer[37] whereas peroxidase enzymes are reported to bring about SET oxidations[38] and iron porphyrins can catalyse both types of reaction.[39] The dye radicals formed in the SET steps subsequently react further by oxidation or disproportionation[40] to give dye cations which, following reaction with H_2O–OH^-, lead to the cleavage of the azo compound and dye bleaching.[38] A programme of research aimed identifying the dye oxidation products is currently underway to provide further confirmation for these mechanisms.

Experimental

Instrumentation

UV-Vis spectra and kinetic data were recorded on a Hewlett Packard HP4582A diode array spectrometer, equipped with a multicell sampling system and the data were analysed with a PC using software A.02.05. Positive and negative ion ESI-MS were obtained on a Finnegan LCQ MAT mass spectrometer. EPR spectra of the manganese complexes were acquired on a Bruker ESP 300 spectrometer equipped with an X-band klystron and 100 kHz modulation. Hyperfine splittings were measured directly from the field scan by determination with a Bruker ER 035H gaussmeter, calibrated with an aqueous solution of Fremy's salt, $a(N) = 1.309$ mT. For those experiments involving frozen samples at 77 K, the EPR sample tube was placed in the EPR cavity in a Dewar flask containing liquid nitrogen. EPR spectra from spin-trapping experiments were recorded with a JEOL JES-RE1X spectrometer at room temperature in an aqueous flat cell.

Materials

All materials were commercially available and used without further purification unless otherwise stated. All the azo dyes were supplied by Unilever Research, these were organically

pure although they contained <5% NaCl from the purification procedure. 1-Phenylazo-2-hydroxynaphthalene-6-sulfonate (Aldrich) was also purified as described previously.[39] The mono- and di-nuclear manganese catalysts and Me_3TACN were provided by R. Hage (Unilever, Holland). The spin-trap DMPO (Sigma Chemical Co Ltd) was purified before use by stirring an aqueous solution with activated charcoal in the dark for 30 min. The charcoal was removed by filtration and the solution was stored at −20 °C. Deionised water was used throughout this study.

Reaction and kinetic procedures

UV-Vis studies of dye bleaching and hydrogen peroxide decomposition. Solutions of the reactants, other than the hydrogen peroxide, were placed in quartz cuvettes in the thermostated spectrometer (30 °C), and after they had reached thermal equilibrium the reactions were initiated by the addition of the oxidant. The dye bleaching kinetics were followed by monitoring the decrease in main visible absorption band of the dye at 4 min intervals.

The hydrogen peroxide content of the reaction mixtures was obtained following a literature procedure.[41] This involved converting the hydrogen peroxide by reaction with iodide into a triiodide anion, the concentration of which was measured spectrophotometrically at 352 nm. The method was calibrated with standard solutions of hydrogen peroxide. Using this method, it was possible to remove aliquots, with a Gilson automatic pipette, from the cuvettes above at timed intervals and quench them in a solution containing potassium iodide, ammonium heptamolybdate, sodium hydroxide and potassium hydrogenphthalate. At the end of the reaction the absorbance of the triiodide anion in each aliquot was used to obtain the concentration of unreacted hydrogen peroxide.

EPR spin-trapping. The reaction solutions were deoxygenated with nitrogen before the addition of hydrogen peroxide and DMPO or DEPMPO. The resultant mixture was pipetted into the EPR flat cell and the scanning of the spectrum was initiated. Typically the time between mixing and scanning was 80 s.

EPR spectra recorded at 77 K. The reaction mixtures were prepared in sample tubes and after the required reaction time, methanol was added (to give an overall concentration of 30% w/w). The solutions were then immediately frozen in liquid nitrogen at 77 K and transferred to the EPR spectrometer.

ESI-MS studies. The reactants were mixed in a thermostated sample tube (30 °C) and the hydrogen peroxide was added. At timed intervals, an aliquot (250 μl) was removed with a syringe and introduced into the mass spectrometer using a syringe pump at rates varying from 3–60 μl min^{-1}. Data recording was started *ca*. 30 s after the start of the infusion, when the ESI-MS signal had stabilised.

Acknowledgements

We thank Unilever Research and the University of York for research studentship funding. We also thank Dr A. C. Whitwood for his assistance with EPR spectroscopy, Dr T. A. Dransfield for his help in running the ESI-MS experiments and Dr R. Hage (Unilever Research, Vlaardingen) for very helpful discussions on the reaction mechanisms. We are grateful to Unilever Research for supplying some of the azo dyes used in this study.

References

1 (*a*) B. Kok, B. Forbusch and M. McGloin, *Photochem. Photobiol.*, 1970, **11**, 457; (*b*) *Manganese redox enzymes*, ed. V. L. Pecoraro, VCH, New York, 1992; (*c*) W. Liang, M. J. Latimer, H. Dau, T. A. Roelofs, K. Sauer and M. P. Klein, *Biochem.*, 1994, **33**, 4923.
2 (*a*) G. C. Dismukes and T. Siderer, *Proc. Natl. Acad. Sci. USA*, 1981, **78**, 274; (*b*) V. V. Barynin and A. I. Grebenko, *Dokl. Akad. Nauk. SSSR*, 1986, **286**, 461.
3 (*a*) Y. Naruta and K. Maryama, *J. Am. Chem. Soc.*, 1991, **113**, 3595; (*b*) E. J. Larson and V. L. Pecoraro, *J. Am. Chem. Soc.*, 1991, **113**, 3810; (*c*) U. Bossek, M. Sahar, T. Weyhermuller and K. Wieghardt, *J. Chem. Soc., Chem. Commun.*, 1992, 1780; (*d*) V. L. Pecoraro, M. J. Baldwin and A. Gelasco, *Chem. Rev.*, 1994, **94**, 807; (*e*) C. Higuchi, H. Sakiyama, H. Okawa and D. E. Fenton, *J. Chem Soc., Dalton, Trans.*, 1995, 4015.
4 (*a*) P. J. Pessiki, S. V. Khangulov, D. M. Ho and G. C. Dismukes, *J. Am. Chem. Soc.*, 1994, **116**, 898; (*b*) P. J. Pessiki and G. C. Dismukes, *J. Am. Chem. Soc.*, 1994, **116**, 898.
5 (*a*) K. Wieghardt, U Bossek and W. Gebert, *Angew. Chem., Int. Ed., Eng.*, 1983, **22**, 328; (*b*) K. Wieghardt, U. Bossek, B. Nuber and J. Weiss, *Inorg. Chim. Acta*, 1987, **126**, 39; (*c*) K. Wieghardt, U. Bossek, B. Nuber, J. Weiss, J. Bonvoisin, M. Corbella, S. E. Vitols and J. J. Girerd, *J. Am. Chem. Soc.*, 1988, **110**, 7398; (*d*) K. Wieghardt, *Angew. Chem., Int. Ed. Eng.*, 1989, **28**, 1153; U. Bossek, T. Weyermuller, B. Nuber, J. Weiss and K. Wieghardt, *J. Am. Chem. Soc.*, 1990, **112**, 6387; (*e*) K. Wieghardt, J Weiss and U. Bossek, *Inorg. Chem.*, 1991, **30**, 4397; (*f*) R. Hage, E. A. Gunnewegh, J. Niel, F. S. B. Tjon, T. Weymuller and K. Wieghardt, *Inorg. Chim. Acta*, 1998, **268**, 43.
6 (*a*) R. Hage, *Rec. Trav. Chim. Pays-Bas*, 1996, **115**, 385; (*b*) R. Hage, J. E. Iburg, J. Kerschner, J. H. Koek, E. L. M. Lempers, R. J. Martens, U. S. Racherla, S. W. Russell, T. Swarthoff, M. R. P. van Vliet, J. B. Warnaar, L. van der Wolf and B. Krijnen, *Nature*, 1994, **246**, 265.
7 D. E. De Vos and T. Bein, *J. Organomet. Chem.*, 1996, **520**, 195.
8 J. Brinksma, L. Schmieder, G. van Vliet, R. Boaron, R. Hage, D. E. De Vos, P. L. Alsters and B. L. Feringa, *Tetrahedron Lett.*, 2002, **43**, 2619.
9 J. R. Lindsay Smith and G. B. Shul'pin, *Tetrahedron Lett.*, 1998, **39**, 4909.
10 B. C. Gilbert, N. W. J. Kamp, J. R. Lindsay Smith and J. Oakes, *J. Chem. Soc., Perkin Trans. 2*, 1997, 2161.
11 C. Zondervan, R. Hage and B. L. Feringa, *J. Chem. Soc., Chem. Commun.*, 1997, 419.
12 D. H. R. Barton, W. Li and J. A. Smith, *Tetrahedron Lett.*, 1998, **39**, 7055.
13 T. Kobayashi, K. Tsuchiya and Y. Nishida, *J. Chem. Soc., Dalton Trans.*, 1996, 2391.
14 D. E. De Vos, J. L. Meinershagen and T. Bein, *Angew. Chem., Intl. Ed.*, 1996, **35**, 2211.
15 J. F. Boe, J. J. Girerd, C. Guignard, J. L. Seris, J. B. Verlac, Patent WO 94 00234, 1994.
16 K. Srivinasan, P. Michaud and J. K. Kochi, *J. Am. Chem. Soc.*, 1986, **108**, 3309; E. N. Jacobsen, in *Comprehensive organometallic chemistry II*, eds G. Wilkinson, F. G. A. Stone, E. W. Abel and L. S. Hegedus, Pergamon, New York, 1995, vol. 12, ch. 11; T. Katsuki, *Coord. Chem. Rev.*, 1995, **140**, 189; C. L. Hill and B. C. Schardt, *J. Am. Chem. Soc.*, 1980, **102**, 6374; J. T. Groves, W. J. Kruper and R. C. Haushalter, *J. Am. Chem. Soc.*, 1980, **102**, 6377; B. Meunier, *Chem. Rev.*, 1992, **92**, 1411.
17 D. Feichtinger and D. A. Plattner, *Angew. Chem., Int. Ed.*, 1997, **36**, 1718; J. T. Groves, J. Lee and S. S. Marla, *J. Am. Chem. Soc.*, 1997, **119**, 6269.
18 D. H. R. Barton, S.-Y. Choi, B. Hu and J. A. Smith, *Tetrahedron*, 1998, **54**, 3367.
19 B. C. Gilbert, N. W. J. Kamp, J. R. Lindsay Smith and J. Oakes, *J. Chem. Soc., Perkin Trans. 2*, 1998, 1841.
20 V. C. Quee-Smith, L. DelPizzo, S. H. Jureller, J. L. Kerschner and R. Hage, *Inorg.Chem.*, 1996, **35**, 6461.
21 J. Oakes, P. Gratton, R. Clark and I. Wilkes, *J. Chem. Soc., Perkin Trans. 2*, 1998, 2569.
22 J. Oakes and P. Gratton, *J. Chem. Soc., Perkin Trans. 2*, 1998, 1857.
23 J. Oakes, G. Welch and P. Gratton, *J. Chem. Soc., Dalton Trans.*, 1997, 3811.
24 J. Oakes, P. Gratton and I. Weil, *J. Chem. Soc., Dalton Trans.*, 1997, 3805.
25 A. R. Forrester and S. P. Hepburn, *J. Chem. Soc. (C)*, 1971, 701.
26 (*a*) L. Eberson, *J. Chem. Soc., Perkin Trans. 2*, 1992, 1807; (*b*) S. Bhattacharjee, M. N. Khan, H. Chandra and M. C. R. Symons, *J. Chem. Soc., Perkin Trans. 2*, 1996, 2631; (*c*) L. Eberson, J. J. MacCullough and O. Persson, *J. Chem. Soc., Perkin Trans. 2*, 1997, 133.
27 J. L. Clement, B. C. Gilbert, W. F. Ho, N. D. Jackson, M. S. Newton, S. Silvester, G. S. Timmins, P. Tordo and A. C. Whitwood, *J. Chem. Soc., Perkin Trans. 2*, 1998, 1715.

28 C. A. Audeh and J. R. Lindsay Smith, *J. Chem. Soc. B*, 1970, 1280; J. R. Lindsay Smith and L. A. V. Mead, *J. Chem. Soc., Perkin Trans. 2*, 1973, 206; J. R. Lindsay Smith and D. Masheder, *J. Chem. Soc., Perkin Trans. 2*, 1976, 47.
29 J. F. Coen, A. T. Smith, L. P. Candeias and J. Oakes, *J. Chem. Soc., Perkin Trans. 2*, 2001, 2125.
30 M. S. Newton and R. Hage, unpublished results.
31 R. Banerjee, B. Mondal and S. Kundu, *J. Chem. Soc., Dalton Trans.*, 1997, 4341.
32 T. E. Jones and R. P. Hamm, *Inorg.Chem.*, 1974, **13**, 1940.
33 M. P. Heyward and C. F. Wells, *J. Chem. Soc., Faraday Trans. 1*, 1988, **84**, 3805.
34 (*a*) G. Davies, L. J. Kirschenbaum and K. Kustin, *Inorg. Chem.*, 1968, **7**, 146; (*b*) C. F. Wells and D. Mays, *J. Chem. Soc. (A)*, 1968, 665.
35 H. B. Dunford, in *Peroxidases in chemistry and biochemistry*, ed. J. Everse, K. E. Everse, and M. B. Grisham, CRC Press, Boca Raton, 1991, vol. 2, p. 1.
36 B. Meunier, in *Biomimetic oxidations catalyzed by transition metal complexes*, ed. B. Meunier, Imperial College Press, London, 2000, p. 171.
37 (*a*) G. M. Badger and G. E. Lewis, *J. Chem. Soc.*, 1953, 2151; (*b*) N. A. Johnson and E. S. Gould, *J. Org. Chem.*, 1974, **39**, 409.
38 (*a*) J. T. Spadaro and V. Renganathan, *Arch. Biochem.*, 1994, **312**, 301; (*b*) S. Goszczynski, A. Paszczynski, M. B. Pasti-Grigsby, R. L. Crawford and D. L. Crawford, *J. Bacteriol.*, 1994, **176**, 1339.
39 G. R Hodges, J. R. Lindsay Smith and J. Oakes, *J. Chem. Soc., Perkin Trans. 2*, 1998, 617.
40 K. K. Sharama, B. S. M. Rao, H. Mohan, J. P. Mittal, J. Oakes and P. O'Neil, *J. Phys. Chem. A*, 2002, **106**, 2915.
41 J. E. Frew, P. Jones and G. Scholes, *Anal. Chim. Acta*, 1983, **155**, 139.